Opto-Electronic Advances

Supplementary information

2019, Vol. 2, No. 5

DOI: 10.29026/oea.2019.190008

Large Rabi splitting obtained in Ag-WS_2 strong-coupling heterostructure with optical microcavity at room temperature

Bowen Li[1†], Shuai Zu[1†], Zhepeng Zhang[2], Liheng Zheng[1], Qiao Jiang[1], Bowen Du[1], Yang Luo[1], Yongji Gong[3], Yanfeng Zhang[2], Feng Lin[1], Bo Shen[1], Xing Zhu[1], Pulickel M. Ajayan[3] and Zheyu Fang[1,4*]

[1]School of Physics, State Key Laboratory for Mesoscopic Physics, Academy for Advanced Interdisciplinary Studies, and Nano-optoelectronics Frontier Center of Ministry of Education, Peking University, Beijing 100871, China; [2]Department of Materials Science and Engineering, College of Engineering, Peking University, Beijing 100871, China; [3]Department of Materials Science and NanoEngineering, Rice University, 6100 Main Street, Houston, TX 77005, USA; [4]Collaborative Innovation Center of Quantum Matter, Beijing 100871, China.

* Correspondence: Z Y Fang, E-mail: zhyfang@pku.edu.cn

This file includes:

Supplementary information for this paper is available at https://doi.org/10.29026/oea.2019.190008

© 2019 Institute of Optics and Electronics, Chinese Academy of Sciences. All rights reserved.

Section 1: Figures S1–S6

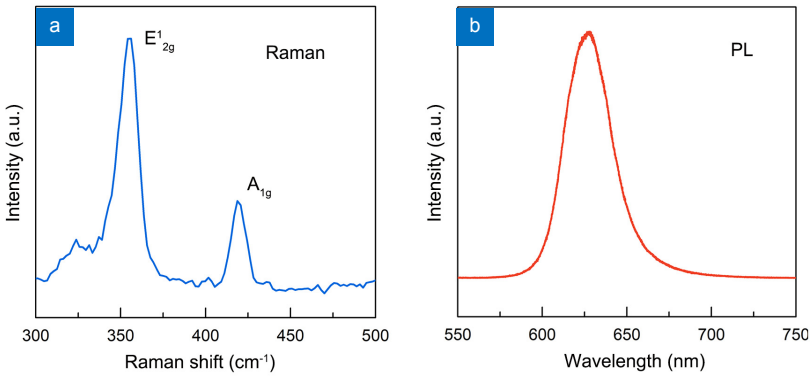

Fig. S1 | Basic characterization of WS_2 monolayers on the Ag-MgF_2 substrate. (**a**) Raman spectrum of the tested WS_2 monolayers, where the in-plane (E^1_{2g}) and out-of-plane (A_{1g}) Raman modes appear at 354 and 416 cm^{-1}, respectively. (**b**) PL spectrum of the WS_2 monolayers on the MgF_2/Ag substrate, which shows a strong emission peak at ~625 nm. Both Raman and PL spectra are in good agreement with the properties of WS_2 monolayers.

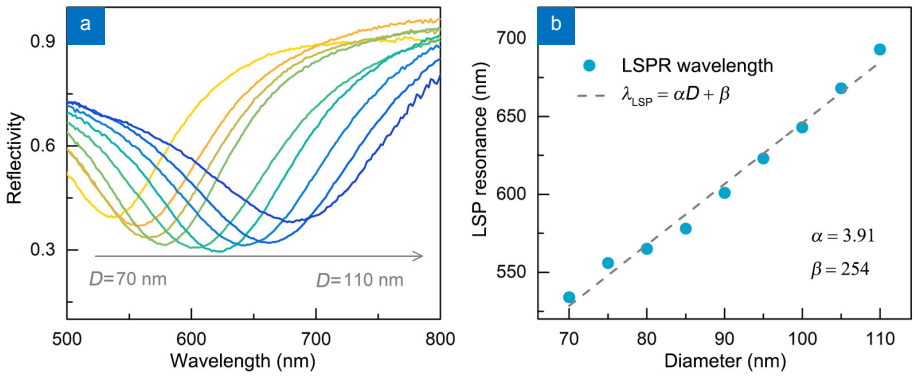

Fig. S2 | Reflectivity spectra of bare Ag nanodisk arrays on the Ag-MgF_2 substrate. (**a**) Normalized reflectivity spectra of bare Ag nanodisk arrays with the diameter increased from 70 nm to 110 nm. (**b**) Localized surface plasmon resonance as a function of nanodisk diameter, which shows a linear dependence of $\lambda_{LSP} = \alpha D + \beta$ with $\alpha = 3.91$ and $\beta = 254$.

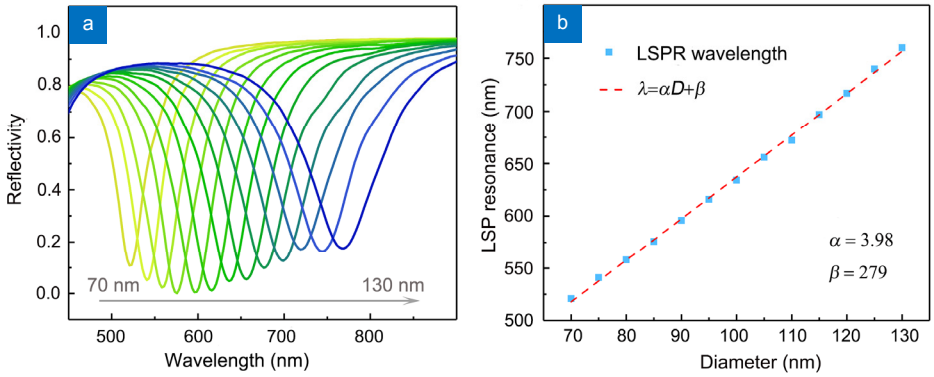

Fig. S3 | FDTD simulation results of bare Ag nanodisk arrays on the Ag-MgF_2 substrate. (**a**) Reflection spectra of different radius of Ag nanodisk varied from 70 nm to 130 nm with a 2.5 nm step were calculated using the FDTD solution, which agrees well with the experimental data. (**b**) Localized surface plasmon resonance vs nanodisk radius showing a linear dependence. The wavelengths of reflection peak were extracted in (a) and such a linear approximation result demonstrates that the energy of localized surface plasmon changes linearly with the increasing nanodisk radius in visible spectrum and the same behavior between experimental data and simulation results also show our accurate nanofabrication.

© 2019 Institute of Optics and Electronics, Chinese Academy of Sciences. All rights reserved.

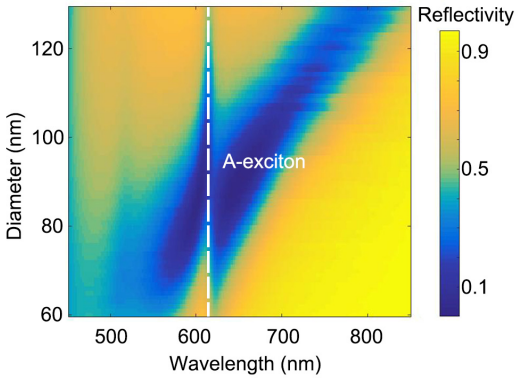

Fig. S4 | The simulated size-dependent dispersion relation of exciton–plasmon in Ag-WS_2 heterostructure by FDTD solutions. Two prominent resonance modes can be identified as the lower (LPB) and upper plexciton branch (UPB), and Rabi splitting was observed with the plasmon resonance of the Ag nanodisk getting closer to the excitons of WS_2 monolayers at 610 nm, which is consistent with our measurements.

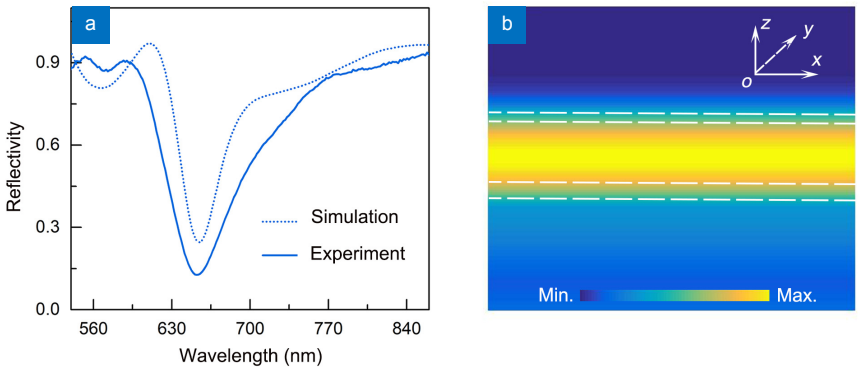

Fig. S5 | Characterization of the optical microcavity. (**a**) The experimental (blue solid curve) and simulated (blue dashed curve) normal-incidence reflection spectrum for the microcavity without Ag-WS_2 hybridstructure. Both experimental and simulated results display a reflection dip ~650 nm, which correspond to the resonance wavelength of the microcavity. (**b**) Normalized electric field intensity distribution $(E/E_{in})^2$ on the *xoz* plane for the optical cavity mode. White dashed lines denote the cross section of the structure.

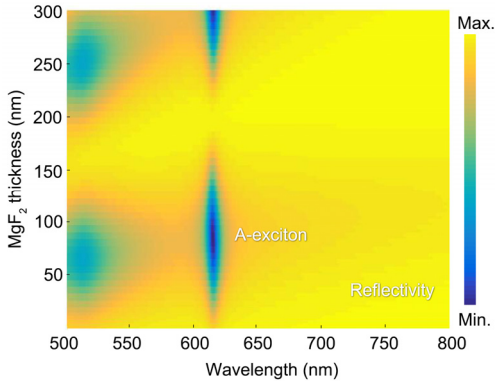

Fig. S6 | The optical reflection of WS_2 monolayers for different MgF_2 film thickness was analyzed by FDTD simulation. All the substrates with 30–120 nm and 270–300 nm MgF_2 film show the dramatic enhancement of absorption features. The substrate with 30 nm MgF_2 and 100 nm Ag was chosen to enhance the optical absorption of WS_2 monolayers.

© 2019 Institute of Optics and Electronics, Chinese Academy of Sciences. All rights reserved.

Section 2: Calculations of the strong coupling in three coupled oscillators

When the Ag-WS_2 heterostructure was embedded into the optical microcavity, the strong plasmon-exciton-cavity interaction occurs with the illumination of incident light. The three-coupled oscillator model was introduced to describe the strong plasmon-exciton-cavity interaction behavior. The plasmon of Ag nanodisk arrays, A-excitons in WS_2 monolayers, and the optical microcavity can be assumed as three oscillators. In the experiment, because the optical microcavity mode is designed far away from the A-exciton of WS_2 monolayers, only plasmon-exciton and plasmon-cavity oscillators are connected, and there is no direct coupling between the exciton and cavity photon to generate traditional polaritons. Therefore, the Hamiltonian of this three-coupled system can be written as:

$$\hat{H}=\hbar\begin{bmatrix} U_{\rm pl}-{\rm i}\dfrac{\gamma_{\rm pl}}{2} & g_{\rm MC} & g_{\rm X} \\ g_{\rm MC} & U_{\rm MC}-{\rm i}\dfrac{\gamma_{\rm MC}}{2} & 0 \\ g_{\rm X} & 0 & U_{\rm X}-{\rm i}\dfrac{\gamma_{\rm X}}{2} \end{bmatrix}, \tag{1}$$

where $\gamma_{\rm pl}$, $\gamma_{\rm X}$, and $\gamma_{\rm MC}$ are the linewidths of plasmon, exciton, and microcavity modes, $U_{\rm pl}$, $U_{\rm X}$, and $U_{\rm MC}$ are the resonance energies of plasmon, exciton, and microcavity modes, while $g_{\rm X}$ and $g_{\rm MC}$ represent plasmon-exciton and plasmon-microcavity interaction constants.

The composition of hybrid states can be modeled by diagonalizing the Hamiltonian of the coupled system. The diagonalization of these Hamiltonians yields new eigenfrequencies and Hopfield coefficients, which represent the contribution of plasmons, microcavity, and excitons to each state. The splitting between each of two branches depends on both plasmon-exciton ($g_{\rm X}$) and plasmon-microcavity ($g_{\rm MC}$) coupling strengths, as well as the resonant frequency and linewidths of all contributing parts, resulting in no simple analytical expressions for eigenfrequencies. As a consequence, there is no simple criteria for the strong coupling in this three-coupled oscillator.

Analogous to the case of strong coupling in two coupled oscillators, the criterion of strong coupling in three oscillators can be derived by the following formula:

$$\Omega=W_{\rm Upper}\gamma_{\rm Upper}+W_{\rm Middle}\gamma_{\rm Middle}+W_{\rm Lower}\gamma_{\rm Lower}\ , \tag{2}$$

where, the $W_{\rm Upper}$, $W_{\rm Middle}$, and $W_{\rm Lower}$ are respectively the weight of each hybrid branch in strong plasmon-exciton-cavity coupling. $\gamma_{\rm Upper}$, $\gamma_{\rm Middle}$ and $\gamma_{\rm Lower}$ are the linewidth of each hybrid branch.

The weight of each hybrid branch in strong plasmon-exciton-cavity coupling can be calculated as follows:

$$\begin{cases} W_{\rm Upper}=\gamma_{\rm Upper}/(\gamma_{\rm Upper}+\gamma_{\rm Middle}+\gamma_{\rm Lower})=28.8\% \\ W_{\rm Middle}=\gamma_{\rm Middle}/(\gamma_{\rm Upper}+\gamma_{\rm Middle}+\gamma_{\rm Lower})=28.8\% \\ W_{\rm Lower}=\gamma_{\rm Lower}/(\gamma_{\rm Upper}+\gamma_{\rm Middle}+\gamma_{\rm Lower})=42.4\% \end{cases}. \tag{3}$$

According to different fraction of three modes in each hybrid branch at diameter = 99 nm shown in Fig. 4(c), the linewidth of hybrid branches can be written as follows:

$$\begin{cases} \gamma_{\rm Upper}=34\%\gamma_{\rm pl}+10\%\gamma_{\rm MC}+56\%\gamma_{\rm X} \\ \gamma_{\rm Middle}=24\%\gamma_{\rm pl}+38\%\gamma_{\rm MC}+38\%\gamma_{\rm X} \\ \gamma_{\rm Lower}=42\%\gamma_{\rm pl}+52\%\gamma_{\rm MC}+6\%\gamma_{\rm X} \end{cases}, \tag{4}$$

Putting equation (3) and equation (4) into equation (2), the contribution of each component (plasmon, exciton, and cavity) in strong plasmon-exciton-microcavity coupling can be obtained, Therefore, the criterion of strong coupling in three coupled oscillators can be written as $\Omega>34.5\%\gamma_{\rm pl}+35.9\%\gamma_{\rm MC}+29.6\%\gamma_{\rm X}$.

Through the peak fitting software, the experimental results in Figs. 1(d), 2(d) and 2(e) were fitted in the Lorentzian shape. And then full widths at half maximum of the corresponding reflection spectra were given by the peak fitting software. The linewidths of plasmon ($\gamma_{\rm pl}\approx$320 meV), cavity ($\gamma_{\rm MC}\approx$150 meV) and exciton ($\gamma_{\rm X}\approx$50 meV) modes can be obtained by the above method. By putting the parameters above into the criterion, the obtained Rabi splitting ($\Omega\approx$300 meV) is satisfied with the strong coupling criterion, where $\Omega>34.5\%\gamma_{\rm pl}+35.9\%\gamma_{\rm MC}+29.6\%\gamma_{\rm X}$, which demonstrates that the strong plasmon-exciton polaritonic hybrid state is successfully generated by combining the Ag-WS_2 heterostructure with the optical microcavity.

© 2019 Institute of Optics and Electronics, Chinese Academy of Sciences. All rights reserved.